HHS Public Access

Author manuscript

J Biomech. Author manuscript; available in PMC 2018 August 16.

Published in final edited form as:

J Biomech. 2017 August 16; 61: 199–207. doi:10.1016/j.jbiomech.2017.07.011.

Crosslinked elastic fibers are necessary for low energy loss in the ascending aorta

Jungsil Kim[1], **Marius Catalin Staiculescu**[1], **Austin J. Cocciolone**[1], **Hiromi Yanagisawa**[2], **Robert P. Mecham**[3], and **Jessica E. Wagenseil**[1]

[1]Dept. of Mechanical Engineering and Materials Science, Washington University, St. Louis, MO

[2]Life Science Center of Tsukuba Advance Research Alliance, University of Tsukuba, Japan

[3]Dept. of Cell Biology and Physiology, Washington University, St. Louis, MO

Abstract

In the large arteries, it is believed that elastin provides the resistance to stretch at low pressure, while collagen provides the resistance to stretch at high pressure. It is also thought that elastin is responsible for the low energy loss observed with cyclic loading. These tenets are supported through experiments that alter component amounts through protease digestion, vessel remodeling, normal growth, or in different artery types. Genetic engineering provides the opportunity to revisit these tenets through the loss of expression of specific wall components. We used newborn mice lacking elastin ($Eln^{-/-}$) or two key proteins (lysyl oxidase, $Lox^{-/-}$, or fibulin-4, $Fbln4^{-/-}$) that are necessary for the assembly of mechanically-functional elastic fibers to investigate the contributions of elastic fibers to large artery mechanics. We determined component content and organization and quantified the nonlinear and viscoelastic mechanical behavior of $Eln^{-/-}$, $Lox^{-/-}$, and $Fbln4^{-/-}$ ascending aorta and their respective controls. We confirmed that the lack of elastin, fibulin-4, or lysyl oxidase leads to absent or highly fragmented elastic fibers in the aortic wall and a 56 – 97% decrease in crosslinked elastin amounts. We found that the resistance to stretch at low pressure is decreased only in $Eln^{-/-}$ aorta, confirming the role of elastin in the nonlinear mechanical behavior of the aortic wall. Dissipated energy with cyclic loading and unloading is increased 53 – 387% in $Eln^{-/-}$, $Lox^{-/-}$, and $Fbln4^{-/-}$ aorta, indicating that not only elastin, but properly assembled and crosslinked elastic fibers, are necessary for low energy loss in the aorta.

Keywords

elastin; fibulin-4; lysyl oxidase; aorta; vascular mechanics; extracellular matrix; collagen

Corresponding Author: Jessica E. Wagenseil, D.Sc., Department of Mechanical Engineering and Materials Science, Washington University, One Brookings Dr., CB 1185, St. Louis, MO 63130, Ph: 314-935-5052, Fax: 314-935-4014, jessica.wagenseil@wustl.edu.

Conflict of Interest Statement

None.

Introduction

Charles Roy published what is likely the first study on the mechanical behavior of large, elastic arteries (Roy 1880). He observed that arteries had maximum distensibility near physiological pressures and became less distensible at higher pressures. Roach and Burton attributed this nonlinear mechanical behavior to the unique combination of elastin and collagen fibers in the arterial wall by selectively digesting each component with proteases (Roach and Burton 1957). They concluded “that the resistance to stretch at low pressures was almost entirely due to elastin fibers, that at physiological pressures due to both collagenous and elastin fibers, but dominantly to collagen, and that at high pressures almost entirely due to collagenous fibers”. “Elastin fibers” are composed mostly of the protein elastin, but are associated with dozens of additional proteins (Kielty et al. 2002). We refer to them by the more general term “elastic fibers”. Numerous studies have used similar protease digestion methods to obtain data supporting Roach and Burton’s observations (Dobrin and Canfield 1984; Fonck et al. 2007; Shadwick 1999). When elastic fibers are compromised in disease or aging, collagen fibers may contribute to the resistance to stretch at lower pressures, stiffening the aortic wall, and increasing the risk of adverse cardiovascular events (Greenwald 2007).

In addition to nonlinear mechanical behavior, large arteries show viscoelastic behavior characterized by energy loss on loading and unloading that helps dampen traveling pressure waves and prevents resonance (Shadwick 1999). Energy loss is finite, but minimal (15 – 20%), so that most of the stored strain energy imparted during systole is returned as work done on the blood by the arterial wall (Gibbons and Shadwick 1989). Viscoelastic behavior can be broken down into elastic and viscous contributions. It is widely believed that the elastic contribution is due to elastic fibers (Apter 1966), while the viscous contribution is due to smooth muscle cells (SMCs) (Wells et al. 1999) or collagen fibers and proteoglycans (Wang et al. 2013). An increased viscous contribution to the mechanical behavior of the aortic wall is a significant, independent risk factor for coronary artery disease (Taniguchi et al. 2015). Relative elastic and viscous contributions of the wall components have been investigated by comparing mechanical behavior after protease digestion to remove specific components (Zou and Zhang 2011), and in situations where there are changes in component amounts due to remodeling (Wang et al. 2013), normal development (Wells et al. 1999), and in different artery types (Fung 1993).

Previous methods to determine wall component contributions to arterial mechanical behavior have some limitations. Proteases may not be selective for the component of interest or may only partially digest components (Chow et al. 2013). Removing one component after it has been integrated into the arterial wall can alter organization of the remaining components (Fonck et al. 2007). Quantification of components after wall remodeling is complicated by the changes in properties (i.e. degradation, crosslinking, waviness, and orientation) that occur along with changes in component amounts (Chow et al. 2013; Fonck et al. 2007). Comparison of component amounts and mechanical behavior among different artery types is also complicated by the changes in component properties that are inherent to elastic and muscular arteries that have very different physiologic roles.

Genetic engineering offers an opportunity to investigate the contribution of different wall components to arterial mechanics by completely removing expression and subsequent incorporation of the component of interest. Elastin knockout mice ($Eln^{-/-}$) die soon after birth with arterial tortuosity, stenoses, and thicker, stiffer aortic walls (Li et al. 1998; Wagenseil et al. 2009). $Eln^{-/-}$ mice represent a model where elastic fibers are not and never have been present to contribute to arterial mechanics. Two of the proteins associated with elastic fibers, lysyl oxidase (LOX) and fibulin-4 (FBLN4), are critical for elastic fiber assembly and are necessary for postnatal survival in mice. $Lox^{-/-}$ and $Fbln4^{-/-}$ mice die soon after birth with arterial tortuosity, aneurysms, and have highly disrupted elastic fibers in the aortic walls (Hornstra et al. 2003; Mäki et al. 2002; Huang et al. 2010; Kim et al. 2015; McLaughlin et al. 2006). LOX crosslinks elastic and collagen fibers, hence $Lox^{-/-}$ mice represent a model where the mechanical contribution of these two major components is altered. FBLN4 interacts with LOX (Horiguchi et al. 2009), and is important for elastic (McLaughlin et al. 2006) and collagen (Papke et al. 2015) fiber assembly and crosslinking, so $Fbln4^{-/-}$ mice represent an additional model where elastic and collagen fiber mechanical contributions are altered. We used aortas from newborn $Eln^{-/-}$, $Lox^{-/-}$, and $Fbln4^{-/-}$ mice and their respective wild-type (WT) controls to revisit two major tenets of large artery mechanics: 1) Resistance to stretch is due to elastic fibers at low pressure and collagen fibers at high pressure; and 2) Elastic fibers are responsible for low energy loss with cyclic loading and unloading.

Materials and Methods

Animals

$Eln^{+/-}$ (Li et al. 1998), $Lox^{+/-}$ (Hornstra et al. 2003), and $Fbln4^{+/-}$ (Huang et al. 2010) mice were bred to produce the associated wild-type (WT) ($^{+/+}$) and knockout (KO) ($^{-/-}$) pups. *Eln* and *Fbln4* mice are in the C57BL/6 background, while *Lox* mice are in the B6 albino background. Pups were used within 24 hours of birth, euthanized by CO_2 inhalation, and the entire thoracic aorta or the ascending aorta (AA) was removed. As sex is difficult to determine in newborn mice, all pups were used and were not separated by sex. For protein composition studies N = 5 – 6/group, for microstructural studies N = 3 – 5/group, and for mechanical testing N = 6 – 8/group. All animal protocols were approved by the Institutional Animal Care and Use Committee.

Aortic protein composition

Protein composition was determined by quantifying the ratios of desmosine, a crosslink specific to mature elastin, and hydroxyproline, an amino acid abundant in collagen, to the total protein in the aortic wall. The entire thoracic aorta was removed, hydrolyzed in 6 N HCl, dried in a speedvac, and then stored at 20°C until use. A competitive ELISA was used to quantify desmosine amounts (Cheng et al. 2013). An ELISA plate was coated with desmosine-ovalbumen conjugate (DOC375, Elastin Products Company), the sample and desmosine antibody (kindly provided by Barry Starcher, University of Texas Health Science Center) were added simultaneously, then secondary peroxidase labeled anti-rabbit IgG (KPL) was added. Hydroxyproline amounts were measured through a Chloramine T reaction (Jamall et al. 1981) and total protein amounts were measured through a ninhydrin assay

(Starcher 2001). Absorbance was determined with a microplate reader and protein amounts were calibrated from a standard curve. Standards were: elastin (E60, Elastin Products Co.), hydroxyproline (H54409, Sigma-Aldrich), and total protein amino acids (012506C, Pickering Labs). Hydroxyproline amounts were converted to collagen amounts assuming that 13.4% of mammalian collagen is hydroxyproline (Neuman and Logan 1950).

Aortic microstructure

AAs were frozen in optimal cutting temperature media immediately after dissection, sectioned on a cryostat, and fluorescently stained to visualize wall microstructure. Alexa Fluor 633 Hydrazide (0.6 μM, Life Technologies) was used for elastin staining (Shen et al. 2012; Clifford et al. 2011). CNA35 (kindly provided by Magnus Hook, Texas A&M) labeled with Oregon Green 488 (Life Technologies) was used for collagen staining (5 μM) (Krahn et al. 2006). Hoechst 34580 (5 μM, Life Technologies) was used for nuclear staining. Images were taken on a Zeiss 710 confocal microscope. $Eln^{+/+}$, $Lox^{+/+}$, and $Fbln4^{+/+}$ AA appeared similar, so representative WT images were used for qualitative comparison to the KO AAs. Cell density was calculated by outlining the cross-sectional wall area and counting cell nuclei per area using Image J software.

Aortic mechanical testing

AAs were stored in physiologic saline solution at 4°C for up to two days before testing (Amin et al. 2011). The AA was mounted in a 37°C Myograph 110P (Danish Myotechnology) bath filled with physiologic saline solution, stretched axially to 1.05 times the unloaded length, and preconditioned by pressurizing for three cycles from 0 – 60 mmHg at a constant rate (4 mmHg/sec). Average AA axial stretch values are 1.17 in newborn $Fbln4^{-/-}$ and $Fbln4^{+/+}$ mice, but are highly variable across individual samples (Kim et al. 2015). Axial stretch at or below the physiologic value provides similar pressure-diameter curves (Wagenseil et al. 2005) and we have noted that newborn aorta is susceptible to axial stretch induced damage, hence we conservatively applied 1.05 axial stretch. The pressure range was chosen based on previous systolic blood pressure measurements averaging 25 mmHg in newborn $Eln^{+/+}$ and 50 mmHg in $Eln^{-/-}$ mice (Wagenseil et al. 2009).

After preconditioning, AAs were pressurized from 0 – 60 mmHg in 5 mmHg increments (7 sec/increment), and then returned from 60 – 0 mmHg at a constant rate (4 mmHg/sec) for three cycles, while recording lumen pressure and outer diameter at 2 Hz. AAs were held at 0 mmHg for 60 sec between cycles. Preliminary experiments with newborn $Eln^{+/+}$ AAs showed that there are no differences in the pressure-outer diameter behavior between the constant rate cycles and those with step increases in pressure, that three preconditioning cycles are sufficient for repeatable behavior, and that the AA returns to a stable unloaded diameter between cycles (Fig. 1). Cross-sectional rings were cut after testing and imaged to determine the AA unloaded thickness. The raw pressure-outer diameter data for loading of $Lox^{+/+}$, $Lox^{-/-}$, $Fbln4^{+/+}$, and $Fbln4^{-/-}$ AA have been previously published (Kim et al. 2015; Staiculescu et al. 2017).

Data analyses

The unloaded thickness (T) was determined by averaging four linear measurements across the wall in three cross-sectional rings for each AA. The unloaded outer diameter (D_o) was determined from the minimum diameter at 0 mmHg from the mechanical testing data. The unloaded inner diameter is $D_i = D_o - 2T$. Unless there was a problem with video tracking of the AA diameter, the third recorded loading-unloading cycle was used for all analyses. The loaded inner diameter (d_i) was calculated from the unloaded dimensions assuming incompressibility (Faury et al. 1999). The average circumferential stretch (λ_θ) was calculated by,

$$\lambda_\theta = \frac{d_i + d_o}{D_i + D_o}. \quad \text{Eqn. 1}$$

The average circumferential Green strain was calculated by,

$$E_\theta = \frac{1}{2}(\lambda_\theta^2 - 1), \quad \text{Eqn. 2}$$

assuming no shear strains.

The average circumferential Cauchy stress (σ_θ) was calculated by,

$$\sigma_\theta = \frac{P d_i}{d_o - d_i}. \quad \text{Eqn. 3}$$

The average circumferential second Piola-Kirchoff stress (S_θ) was calculated by,

$$S_\theta = \frac{\sigma_\theta}{\lambda_\theta^2}. \quad \text{Eqn. 4}$$

Although a thin-walled approximation is not appropriate for newborn mouse aorta because the radius to thickness ratio is approximately three, radial variations in stress and strain were ignored by using the average stress and strain values (Ferruzzi et al. 2013). The calculated Green strain-second Piola-Kirchoff stress curves were numerically integrated using Matlab (Mathworks) to determine the area under the loading and unloading curves. The area under the loading curve (A_L) represents the stored energy with loading and the area under the unloading curve (A_U) represents the returned energy with unloading (Fig. 2A) (Tian et al. 2013). The percent dissipated energy (DE) was calculated by,

$$DE = \frac{A_L - A_U}{A_L} * 100\%. \quad \text{Eqn. 5}$$

The percent dissipated energy is a measure of the energy lost with each cyclic pressurization cycle between 0 – 60 mmHg at 1.05 axial stretch.

Since the AA loading and unloading behavior is repeatable at the constant strain rates after preconditioning, we applied the concept of pseudo-elasticity and separately analyzed the loading and unloading curves (Fung 1993). Two linear functions were fit to the Green strain-second Piola-Kirchoff stress loading or unloading curves by systematically varying the transition point between the functions until the minimum squared error was obtained between the experimental and calculated stresses for each strain using Matlab. The slopes of the resulting functions are called the “low modulus” and “high modulus” and are estimates of the resistance to stretch under low and high pressures, respectively (Fig. 2B). The transition point represents the strain and stress at which it is hypothesized that the aorta transitions from elastin-dominant to collagen-dominant mechanical behavior (Tabima and Chesler 2010).

Statistical analyses

Two outliers (one $Eln^{+/+}$ and one $Fbln4^{+/+}$) were identified in the pressure-outer diameter data using SPSS software (IBM). Examination of the data suggested there may have been a leak during mechanical testing for these AAs, so they were removed from all further analyses. One-way ANOVA followed by a Bonferroni posthoc test for multiple comparisons was used to compare all data using Graphpad (Prism) or SPSS software. $P < 0.05$ was considered significant.

Results

Aortic protein composition and microstructure

Biochemical assays were used to determine the amounts of crosslinked elastin and total collagen in the newborn mouse AA. Crosslinked elastin amounts, measured by desmosine, are reduced 56 – 97% in KO AAs compared to their respective WT controls (Fig. 3A). Total collagen amounts, measured by hydroxyproline, are similar in all groups. Fluorescence microscopy was used to examine the organization of elastin, collagen, and cell nuclei in the newborn mouse AA (Fig. 4). Complete layers of elastic laminae can be seen in WT AA, which are absent in $Eln^{-/-}$ AA and fragmented in $Lox^{-/-}$ and $Fbln4^{-/-}$ AA (Fig. 4A – D). Collagen staining looks relatively normal in all KO AAs, except for the additional layers of collagen associated with additional SMC/elastic fiber layers through the wall in KO AAs (Fig. 4E – H). The density of cell nuclei per unit wall area is similar across groups (not shown), but cell nuclei appear more disorganized in the KO AAs, especially near the lumen (Fig. 4I – L).

Aortic dimensions and mechanical behavior

Unloaded outer diameters at 0 mmHg from the mechanical tests and measured thicknesses from cut cross-sectional rings are shown in Fig. 5. $Fbln4^{-/-}$ AA is 23% larger than $Fbln4^{+/+}$. The unloaded thicknesses of KO AAs are 18 – 45% larger than their respective WT controls. Newborn mouse AA demonstrates nonlinear outer diameter vs. pressure behavior (Fig. 6). $Eln^{-/-}$ AA has smaller diameters than $Eln^{+/+}$, while $Lox^{-/-}$ AA and $Fbln4^{-/-}$ AA have larger

diameters than their respective WT controls for the loading data between 5 – 30 mmHg. The WT AAs show similar diameter-pressure behavior to each other, with slight shifts in the absolute diameter values. The loading and unloading data follow similar paths for each WT group. The loading and unloading data follow different paths for each KO group, with the largest differences between loading and unloading paths observed in $Eln^{-/-}$ AA.

Average circumferential Green strain vs. second Piola-Kirchoff stress data are shown in Fig. 7. Strain energy values were calculated by numerically integrating the strain-stress curves. There are no differences in the stored energy with loading between groups, but the returned energy with unloading is 43 – 69% lower for the KO AAs compared to their respective WT controls (Fig. 8). These differences leads to a 53 – 387% increase in dissipated energy for one pressurization cycle for the KO AAs compared to their respective WT controls. Bilinear functions were fit to the circumferential Green strain vs. second Piola-Kirchoff stress data to quantify and compare the mechanical behavior between groups. The transition Green strain is similar for loading and unloading data for all groups (Fig. 9A). The average transition second Piola-Kirchoff stress is 27 – 72% lower for the KO AAs compared to their respective WT AAs, except for the loading data of $Lox^{-/-}$ AA compared to $Lox^{+/+}$ AA (Fig. 9B). The low modulus is decreased 82% in $Eln^{-/-}$ AA for unloading only (Fig. 9C), while the high modulus is similar in all groups (Fig. 9D).

Table 1 provides a summary of the different mouse models, the crosslinked elastin and total collagen amounts, and the measured changes in aortic mechanical behavior.

Discussion

Newborn $Eln^{-/-}$, $Lox^{-/-}$, and $Fbln4^{-/-}$ mice allow us to revisit basic tenets of how elastic and collagen fibers contribute to the nonlinear, viscoelastic behavior of the aortic wall. Biochemical assays confirm that the absence of elastin expression leads to essentially no crosslinked elastin, while the absence of lysyl oxidase or fibulin-4 expression severely decreases the amount of crosslinked elastin. There are no compensatory increases in total collagen amounts. The protein quantification results are consistent with previous studies (Hornstra et al. 2003; Li et al. 1998; McLaughlin et al. 2006). The fluorescence microscopy images confirm that the lack of elastin, fibulin-4, or lysyl oxidase results in absent or severely disrupted elastic fibers in the aortic wall. The microscopy images suggest changes in cellular organization, but do not show any obvious changes in cell or collagen amount or collagen organization for the KO AAs. The fluorescence microscopy results are consistent with previous data on the aortic microstructure in these mice (Wagenseil et al. 2009; Mäki et al. 2002; Huang et al. 2010; Kim et al. 2015).

Severe defects in elastic fibers are associated with thickening of the aortic wall in newborn mice. Wall thickening may be a remodeling response to altered circumferential stresses during development (Wells et al. 1999), caused by mechanical and hemodynamic changes accompanying the elastic fiber defects. The absence of elastin leads to a smaller AA diameter when pressurized and is consistent with the aortic stenosis phenotype observed in humans with mutations in the elastin gene (Li et al. 1997). The absence of lysyl oxidase or fibulin-4 leads to a larger AA diameter when pressurized and is consistent with the aortic

aneurysm phenotype of humans with mutations in lysyl oxidase (Guo et al. 2016) or fibulin-4 (Hucthagowder et al. 2006). The data show that the absence of elastic fibers vs. improper assembly and crosslinking of elastic fibers have similar effects on the AA wall thickness, but differential effects on the AA diameter-pressure behavior.

Roach and Burton put forth the tenet that the resistance to stretch at low pressure in large arteries is due to elastic fibers (Roach and Burton 1957). Although all three KO mouse models have severe decreases in the amount of crosslinked elastic fibers, only the $Eln^{-/-}$ AA has reduced low modulus values and the low modulus is only significantly different for the unloading data. This indicates that the elastin protein itself, and not necessarily properly assembled and crosslinked elastic fibers, provide the resistance to stretch at low pressures in the newborn mouse aorta. It also highlights the importance of examining both loading and unloading behavior. Our results extend previous studies where arterial elastin is digested with specific proteases (Dobrin and Canfield 1984; Fan et al. 2005; Fonck et al. 2007).

The second part of Roach and Burton's tenet is that the resistance to stretch at high pressure in large arteries is due to collagen fibers (Roach and Burton 1957). Although the absence of lysyl oxidase decreases collagen crosslinking (Hornstra et al. 2003) and fibulin-4 has been implicated in collagen fiber assembly and crosslinking (Papke et al. 2015), we did not see any changes in the high modulus values for $Fbln4^{-/-}$ or $Lox^{-/-}$ AA. Since we found no changes in absolute collagen amounts, our results indicate that other compensatory mechanisms, such as changes in the type, distribution, structure, and crosslinking of different collagen proteins, are in place to maintain the resistance to stretch at high pressure in the absence of lysyl oxidase or fibulin-4.

The transition from elastin-dominant to collagen-dominant mechanical behavior (Tabima and Chesler 2010) occurs at the same Green strain, but lower second Piola-Kirchoff stresses, when elastin is absent from or is improperly assembled and crosslinked in the aortic wall. The nonlinear behavior is usually attributed to wavy collagen fibers that do not begin to bear load until straightened (Fung 1993). Our results suggest that the waviness of the collagen fibers in the aortic wall is similar in KO and WT AAs, so that they begin to bear load at the same strain, but that the reduced amounts of crosslinked elastic fibers present in the KO AAs cannot support the same stress as WT and so collagen fibers begin contributing at lower stresses. The relationship of the transition point to the physiologic loading conditions is critical for determining the *in vivo* behavior of the aortic wall. The second Piola-Kirchoff stress at 25 mmHg, the average systolic pressure in a newborn WT mouse (Wagenseil et al. 2009), is 5 – 10 kPa for all groups, which is in the same range as the transition stress. This indicates that both elastic and collagen fibers contribute to the aortic mechanical behavior at physiologic pressures in newborn mouse AA, as put forth by Roach and Burton (Roach and Burton 1957), and that small changes in the physiologic loading conditions near the transition point can significantly affect the *in vivo* aortic mechanical behavior and consequent cardiovascular function (Greenwald 2007).

KO AAs have significantly increased dissipated energy compared to WT. The large increase is consistent with the tenet that elastic fibers are responsible for low energy loss in the large, elastic arteries. The major component of elastic fibers, elastin, alone is not enough, however,

correctly assembled and crosslinked elastic fibers are necessary for low energy loss. Fluid-structure interaction models show that increased viscous behavior of the arterial wall affects pressure wave dissipation in the cardiovascular tree (Maxwell and Anliker 1968; Ghigo et al. 2017; Perdikaris and Karniadakis 2014). Altered pressure wave dissipation may affect small vessels such as the coronary arteries, as evidenced by a viscoelastic index that is a significant, independent risk factor for coronary artery disease (Taniguchi et al. 2015). *In vitro* studies have shown that elastic and viscoelastic substrate properties can influence cell behavior (Chaudhuri et al. 2015). Hence, viscoelastic properties of the aortic wall may affect cardiovascular function and influence cell-directed remodeling in elastic fiber disease and are an important direction for future work.

The mouse models used in this study have severe elastic fiber defects. Less severe mouse models of elastic fiber defects survive to adulthood and offer additional insight into the role of elastic fibers in arterial mechanics. Elastin haploinsufficient ($Eln^{+/-}$) mice have 60% of the normal elastin levels (Faury et al. 2003), while fibulin-5 knockout ($Fbln5^{-/-}$) mice have normal crosslinked elastin levels, but fragmented elastic fibers (Le et al. 2015). Microstructurally-based constitutive modeling of biaxial mechanical test data suggests that collagen fiber structure or orientation are altered in $Eln^{+/-}$ and $Fbln5^{-/-}$ arteries to maintain circumferential mechanical behavior near WT levels (Cheng et al. 2013; Wan and Gleason 2013). Compensatory remodeling of collagen fibers during development may also play a role in our current study.

In conclusion, we offer two revised tenets of large artery mechanics that highlight the differential contributions of elastin vs. properly assembled and crosslinked elastic fibers: 1) Resistance to stretch is due to elastin at low pressure; and 2) Crosslinked elastic fibers are responsible for low energy loss on loading and unloading. We do not include collagen or cell contributions in our revised tenets at this time, as additional studies are needed to further investigate their roles.

Limitations

We interpret our results in $Eln^{-/-}$, $Lox^{-/-}$, and $Fbln4^{-/-}$ AA to be the result of the absence of properly assembled and crosslinked elastic fibers. Although there were no changes in cell density or total collagen amounts, there could be compensatory changes in other cell or collagen characteristics that contribute to the observed differences in mechanical behavior. Future studies must carefully evaluate contributions of other major wall components. Newborn mouse AA is limited in size and has a natural curvature, so bending moments and end effects may be present during mechanical testing. We evaluated only circumferential mechanical behavior at a single axial stretch ratio within a small range of cyclic loading rates. Future studies should include axial mechanical behavior and a more comprehensive analysis of viscoelastic properties.

Acknowledgments

This study was partially funded by NIH grants HL115560 (J. Wagenseil), HL53325 (R. Mecham), HL106305 (H. Yanagisawa) and HL-105314 (R. Mecham and J. Wagenseil). Tom Broekelmann is acknowledged for assistance with the desmosine assay.

References

Amin M, Kunkel AG, Le VP, Wagenseil JE. Effect of storage duration on the mechanical behavior of mouse carotid artery. J Biomech Eng. 2011; 133(7):071007.doi: 10.1115/1.4004415 [PubMed: 21823746]

Apter JT. Correlation of visco-elastic properties of large arteries with micorscopic structure. Circulation Research XIX. 1966

Chaudhuri O, Gu L, Darnell M, Klumpers D, Bencherif SA, Weaver JC, Huebsch N, Mooney DJ. Substrate stress relaxation regulates cell spreading. Nat Commun. 2015; 6:6364.doi: 10.1038/ncomms7365

Cheng JK, Stoilov I, Mecham RP, Wagenseil JE. A fiber-based constitutive model predicts changes in amount and organization of matrix proteins with development and disease in the mouse aorta. Biomech Model Mechanobiol. 2013; 12(3):497–510. DOI: 10.1007/s10237-012-0420-9 [PubMed: 22790326]

Chow MJ, Mondonedo JR, Johnson VM, Zhang Y. Progressive structural and biomechanical changes in elastin degraded aorta. Biomech Model Mechanobiol. 2013; 12(2):361–372. DOI: 10.1007/s10237-012-0404-9 [PubMed: 22623109]

Clifford PS, Ella SR, Stupica AJ, Nourian Z, Li M, Martinez-Lemus LA, Dora KA, Yang Y, Davis MJ, Pohl U, Meininger GA, Hill MA. Spatial distribution and mechanical function of elastin in resistance arteries - a role in bearing longitudinal stress. Atertio Thromb Vasc Biol. 2011; 31(12): 2889–2896. DOI: 10.1161/ATVBAHA.111.236570

Dobrin PB, Canfield TR. Elastase, collagenase, and the biaxial elastic properties of dog carotid artery. American Journal of Physiology. 1984; 247(1 Pt 2):H124–131. [PubMed: 6331204]

Fan Y, Zhao J, Liao D, Gregersen H. The effect of digestion of collagen and elastin on histomorphometry and the zero-stress state in rat esophagus. Dig Dis Sci. 2005; 50(8):1497–1505. [PubMed: 16110842]

Faury G, Maher GM, Li DY, Keating MT, Mecham RP, Boyle WA. Relation between outer and luminal diameter in cannulated arteries. Am J Physiol. 1999; 277(5 Pt 2):H1745–1753. [PubMed: 10564127]

Faury G, Pezet M, Knutsen RH, Boyle WA, Heximer SP, McLean SE, Minkes RK, Blumer KJ, Kovacs A, Kelly DP, Li DY, Starcher B, Mecham RP. Developmental adaptation of the mouse cardiovascular system to elastin haploinsufficiency. J Clin Invest. 2003; 112(9):1419–1428. [PubMed: 14597767]

Ferruzzi J, Bersi MR, Humphrey JD. Biomechanical phenotyping of central arteries in health and disease: advantages of and methods for murine models. Ann Biomed Eng. 2013; 41(7):1311–1330. DOI: 10.1007/s10439-013-0799-1 [PubMed: 23549898]

Fonck E, Prod'hom G, Roy S, Augsburger L, Rufenacht DA, Stergiopulos N. Effect of elastin degradation on carotid wall mechanics as assessed by a constituent-based biomechanical model. Am J Physiol Heart Circ Physiol. 2007; 292(6):H2754–2763. DOI: 10.1152/ajpheart.01108.2006 [PubMed: 17237244]

Fung, YC. Biomechanics: Mechanical Properties of Living Tissues. 2nd. SpringerVerlag; New York: 1993.

Ghigo AR, Wang XF, Armentano R, Fullana JM, Lagree PY. Linear and Nonlinear Viscoelastic Arterial Wall Models: Application on Animals. J Biomech Eng. 2017; 139(1)doi: 10.1115/1.4034832

Gibbons CA, Shadwick RE. Functional similarities in the mechanical design of the aorta in lower vertebrates and mammals. Experientia. 1989; 45(11–12):1083–1088. [PubMed: 2513219]

Greenwald SE. Ageing of the conduit arteries. The Journal of pathology. 2007; 211(2):157–172. DOI: 10.1002/path.2101 [PubMed: 17200940]

Guo D, Regalado ES, Gong L, Duan X, Santos-Cortez RL, Arnaud P, Ren Z, Cai B, Hostetler EM, Moran R, Liang D, Estrera AL, Safi HJ, Leal SM, Bamshad MJ, Shendure J, Nickerson DA, Jondeau G, Boileau C, Milewicz DM. LOX Mutations Predispose to Thoracic Aortic Aneurysms and Dissections. Circ Res. 2016; doi: 10.1161/CIRCRESAHA.115.307130

Horiguchi M, Inoue T, Ohbayashi T, Hirai M, Noda K, Marmorstein LY, Yabe D, Takagi K, Akama TO, Kita T, Kimura T, Nakamura T. Fibulin-4 conducts proper elastogenesis via interaction with cross-linking enzyme lysyl oxidase. Proc Natl Acad Sci U S A. 2009; 106(45):19029–19034. doi: 0908268106 [pii] 10.1073/pnas.0908268106. [PubMed: 19855011]

Hornstra IK, Birge S, Starcher B, Bailey AJ, Mecham RP, Shapiro SD. Lysyl oxidase is required for vascular and diaphragmatic development in mice. J Biol Chem. 2003; 278(16):14387–14393. [PubMed: 12473682]

Huang J, Davis EC, Chapman SL, Budatha M, Marmorstein LY, Word RA, Yanagisawa H. Fibulin-4 deficiency results in ascending aortic aneurysms: a potential link between abnormal smooth muscle cell phenotype and aneurysm progression. Circ Res. 2010; 106(3):583–592. DOI: 10.1161/CIRCRESAHA.109.207852 [PubMed: 20019329]

Hucthagowder V, Sausgruber N, Kim K, Angle B, Marmorstein L, Urban Z. Fibulin-4: a novel gene for an autosomal recessive cutis laxa syndrome. Am J Hum Genet. 2006; 78(6):1075–1080. DOI: 10.1086/504304 [PubMed: 16685658]

Jamall IS, Finelli VN, Que Hee SS. A simple method to determine nanogram levels of 4-hydroxyproline in biological tissues. Analytical biochemistry. 1981; 112(1):70–75. [PubMed: 7258630]

Kielty CM, Sherratt MJ, Shuttleworth CA. Elastic fibres. Journal of cell science. 2002; 115(Pt 14): 2817–2828. [PubMed: 12082143]

Kim J, Procknow JD, Yanagisawa H, Wagenseil JE. Differences in genetic signaling, and not mechanical properties of the wall, are linked to ascending aortic aneurysms in fibulin-4 knockout mice. Am J Physiol Heart Circ Physiol. 2015; 309(1):H103–113. DOI: 10.1152/ajpheart.00178.2015 [PubMed: 25934097]

Krahn KN, Bouten CV, van Tuijl S, van Zandvoort MA, Merkx M. Fluorescently labeled collagen binding proteins allow specific visualization of collagen in tissues and live cell culture. Analytical biochemistry. 2006; 350(2):177–185. DOI: 10.1016/j.ab.2006.01.013 [PubMed: 16476406]

Le VP, Cheng JK, Kim J, Staiculescu MC, Ficker SW, Sheth SC, Bhayani SA, Mecham RP, Yanagisawa H, Wagenseil JE. Mechanical factors direct mouse aortic remodelling during early maturation. J R Soc Interface. 2015; 12(104):20141350.doi: 10.1098/rsif.2014.1350 [PubMed: 25652465]

Li DY, Brooke B, Davis EC, Mecham RP, Sorensen LK, Boak BB, Eichwald E, Keating MT. Elastin is an essential determinant of arterial morphogenesis. Nature. 1998; 393(6682):276–280. [PubMed: 9607766]

Li DY, Toland AE, Boak BB, Atkinson DL, Ensing GJ, Morris CA, Keating MT. Elastin point mutations cause an obstructive vascular disease, supravalvular aortic stenosis. Human molecular genetics. 1997; 6(7):1021–1028. [PubMed: 9215670]

Mäki JM, Räsänen J, Tikkanen H, Sormunen R, Mäkikallio K, Kivirikko KI, Soininen R. Inactivation of the Lysyl Oxidase Gene Lox Leads to Aortic Aneurysms, Cardiovascular Dysfunction, and Perinatal Death in Mice. Circulation. 2002; 106(19):2503–2509. DOI: 10.1161/01.cir.0000038109.84500.1e [PubMed: 12417550]

Maxwell JA, Anliker M. The dissipation and dispersion of small waves in arteries and veins with viscoelastic wall properties. Biophys J. 1968; 8(8):920–950. DOI: 10.1016/S0006-3495(68)86529-4 [PubMed: 5661901]

McLaughlin PJ, Chen Q, Horiguchi M, Starcher BC, Stanton JB, Broekelmann TJ, Marmorstein AD, McKay B, Mecham R, Nakamura T, Marmorstein LY. Targeted disruption of fibulin-4 abolishes elastogenesis and causes perinatal lethality in mice. Molecular and cellular biology. 2006; 26(5): 1700–1709. [PubMed: 16478991]

Neuman RE, Logan MA. The determination of collagen and elastin in tissues. J Biol Chem. 1950; 186(2):549–556. [PubMed: 14794650]

Papke CL, Tsunezumi J, Ringuette LJ, Nagaoka H, Terajima M, Yamashiro Y, Urquhart G, Yamauchi M, Davis EC, Yanagisawa H. Loss of fibulin-4 disrupts collagen synthesis and maturation: implications for pathology resulting from EFEMP2 mutations. Human molecular genetics. 2015; 24(20):5867–5879. DOI: 10.1093/hmg/ddv308 [PubMed: 26220971]

Perdikaris P, Karniadakis GE. Fractional-order viscoelasticity in one-dimensional blood flow models. Ann Biomed Eng. 2014; 42(5):1012–1023. DOI: 10.1007/s10439-014-0970-3 [PubMed: 24414838]

Roach MR, Burton AC. The reason for the shape of the distensibility curves of arteries. Can J Med Sci. 1957; 35(8):681–690.

Roy CS. Elastic properties of the arterial wall. J Physiol (Lond). 1880; 3:125–159.

Shadwick RE. Mechanical design in arteries. The Journal of experimental biology. 1999; 202(Pt 23): 3305–3313. [PubMed: 10562513]

Shen Z, Lu Z, Chhatbar PY, O'Herron P, Kara P. An artery-specific fluorescent dye for studying neurovascular coupling. Nat Methods. 2012; 9(3):273–276. DOI: 10.1038/nmeth.1857 [PubMed: 22266543]

Staiculescu MC, Kim J, Mecham RP, Wagenseil JE. Mechanical behavior and matrisome gene expression in aneurysm-prone thoracic aorta of newborn lysyl oxidase knockout mice. Am J Physiol Heart Circ Physiol. 2017 accepted.

Starcher B. A ninhydrin-based assay to quantitate the total protein content of tissue samples. Analytical biochemistry. 2001; 292(1):125–129. DOI: 10.1006/abio.2001.5050 [PubMed: 11319826]

Tabima DM, Chesler NC. The effects of vasoactivity and hypoxic pulmonary hypertension on extralobar pulmonary artery biomechanics. J Biomech. 2010; 43(10):1864–1869. DOI: 10.1016/j.jbiomech.2010.03.033 [PubMed: 20416876]

Taniguchi R, Hosaka A, Miyahara T, Hoshina K, Okamoto H, Shigematsu K, Miyata T, Sugiura R, Yokobori AT Jr, Watanabe T. Viscoelastic Deterioration of the Carotid Artery Vascular Wall is a Possible Predictor of Coronary Artery Disease. Journal of atherosclerosis and thrombosis. 2015; 22(4):415–423. DOI: 10.5551/jat.24513 [PubMed: 25399931]

Tian L, Wang Z, Lakes RS, Chesler NC. Comparison of approaches to quantify arterial damping capacity from pressurization tests on mouse conduit arteries. J Biomech Eng. 2013; 135(5): 54504.doi: 10.1115/1.4024135 [PubMed: 24231965]

Wagenseil JE, Ciliberto CH, Knutsen RH, Levy MA, Kovacs A, Mecham RP. Reduced vessel elasticity alters cardiovascular structure and function in newborn mice. Circ Res. 2009; 104(10):1217–1224. DOI: 10.1161/CIRCRESAHA.108.192054 [PubMed: 19372465]

Wagenseil JE, Nerurkar NL, Knutsen RH, Okamoto RJ, Li DY, Mecham RP. Effects of elastin haploinsufficiency on the mechanical behavior of mouse arteries. Am J Physiol Heart Circ Physiol. 2005; 289(3):H1209–1217. [PubMed: 15863465]

Wan W, Gleason RL Jr. Dysfunction in elastic fiber formation in fibulin-5 null mice abrogates the evolution in mechanical response of carotid arteries during maturation. Am J Physiol Heart Circ Physiol. 2013; 304(5):H674–686. DOI: 10.1152/ajpheart.00459.2012 [PubMed: 23241326]

Wang Z, Lakes RS, Golob M, Eickhoff JC, Chesler NC. Changes in large pulmonary arterial viscoelasticity in chronic pulmonary hypertension. PLoS One. 2013; 8(11):e78569.doi: 10.1371/journal.pone.0078569 [PubMed: 24223157]

Wells SM, Langille BL, Lee JM, Adamson SL. Determinants of mechanical properties in the developing ovine thoracic aorta. Am J Physiol. 1999; 277(4 Pt 2):H1385–1391. [PubMed: 10516173]

Zou Y, Zhang Y. The orthotropic viscoelastic behavior of aortic elastin. Biomech Model Mechanobiol. 2011; 10(5):613–625. DOI: 10.1007/s10237-010-0260-4 [PubMed: 20963623]

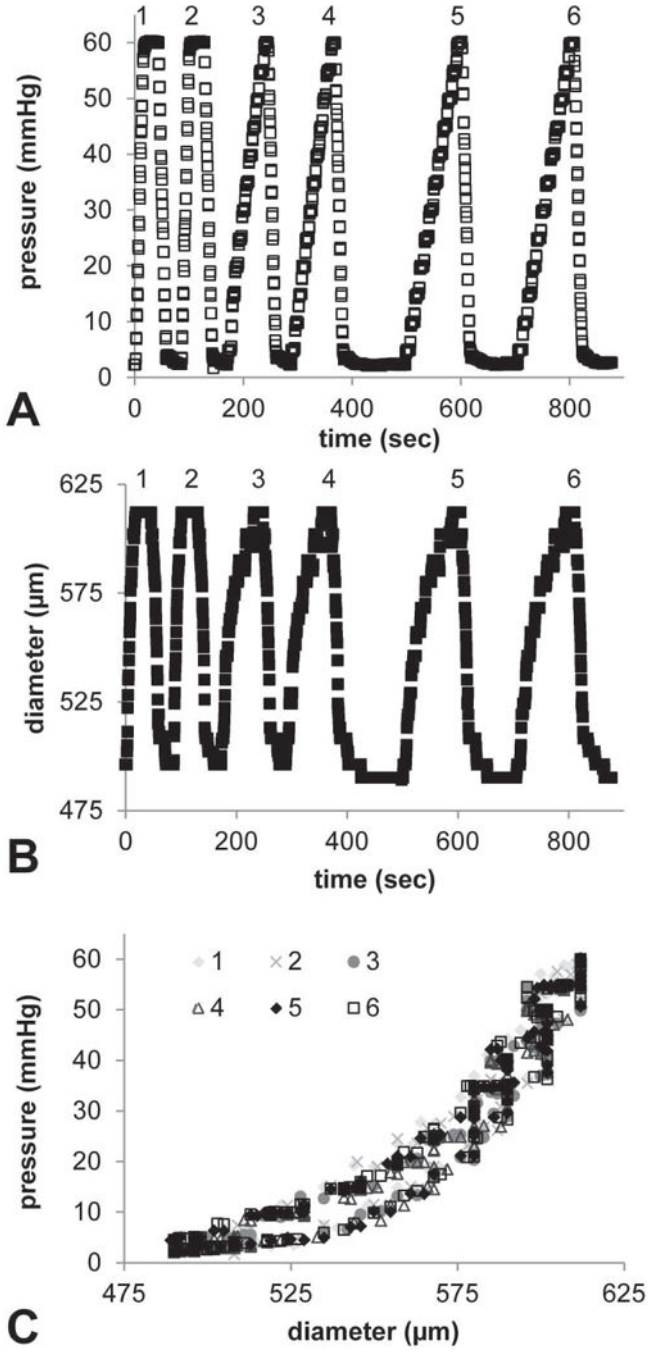

Fig. 1.

Representative preliminary mechanical tests in newborn $Eln^{+/+}$ AA to investigate the effects of pressurization rate and repeatability. Time vs. pressure (A) and time vs. outer diameter (B) show constant loading and unloading rates for the first two cycles, then step pressurization rates for the loading portion only of the next four cycles. After the fourth cycle, a 60 sec wait time was implemented between cycles to allow the diameter to return to a stable unloaded value. The resulting outer diameter-pressure curves (C) do not vary with pressurization rate and are highly repeatable for each cycle number.

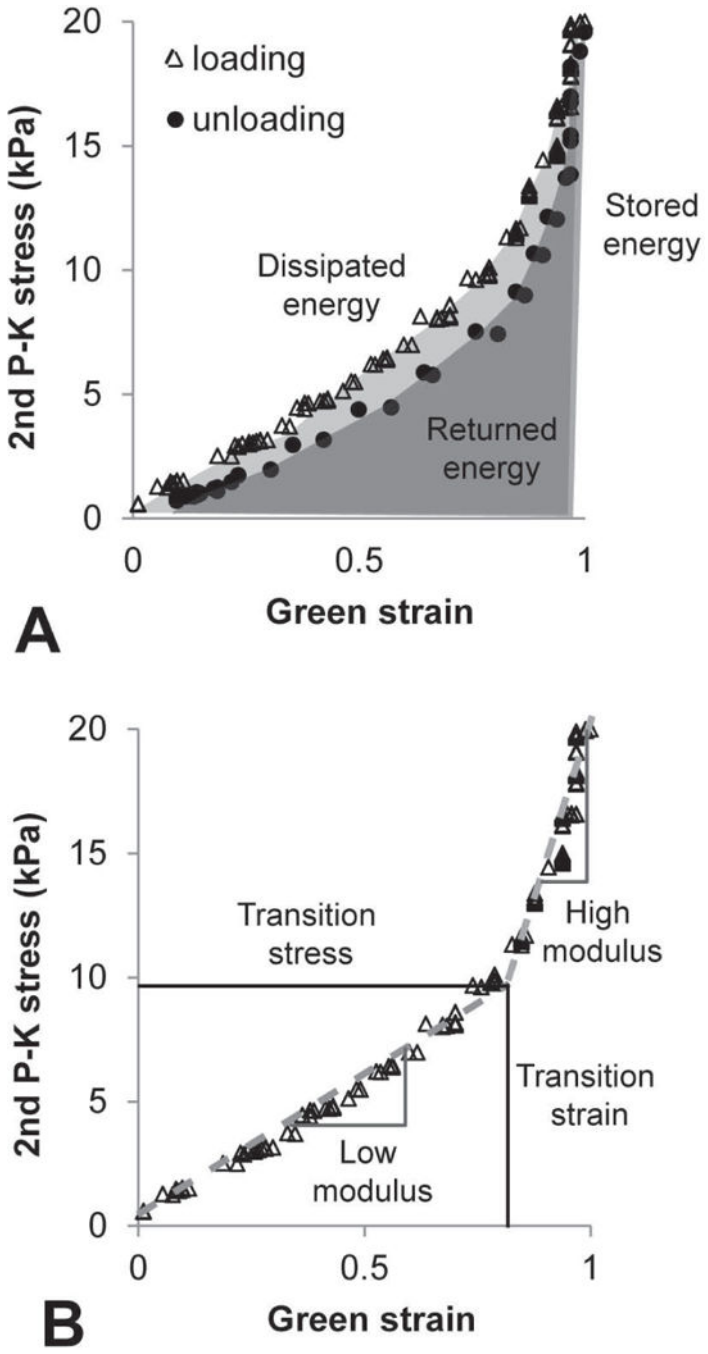

Fig. 2.

Representative circumferential Green strain vs. second Piola-Kirchoff (2nd P–K) stress data for a newborn $Lox^{+/+}$ AA. Loading and unloading data are shown to demonstrate energy calculations (A). Stored energy is the total area under the loading curve (light gray + dark gray). Returned energy is the total area under the unloading curve (dark gray). Dissipated energy is the percent energy lost during one complete loading and unloading cycle (represented by the light gray area). Loading data are shown to demonstrate the transition

strain, transition stress, low modulus, and high modulus calculations (B). Two linear functions were fit to the data and the transition point between the functions was determined.

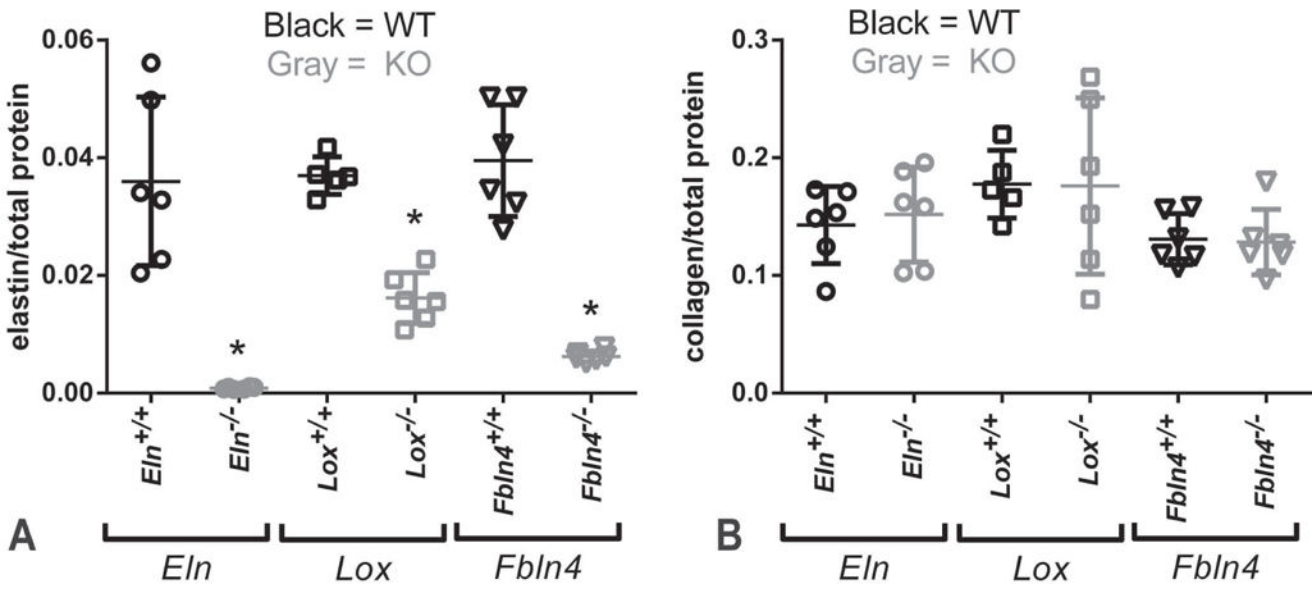

Fig. 3.

Protein composition of newborn mouse AAs. KO AAs have significantly reduced amounts of crosslinked elastin, as measured by a competitive ELISA for desmosine, an elastin-specific crosslink (A). There is no compensatory increase in total collagen amounts, as measured by a reaction with hydroxyproline, an amino acid abundant in collagen (B). * = $P < .05$. Mean ± SD are shown on the scatter plots. N = 5 – 6/group.

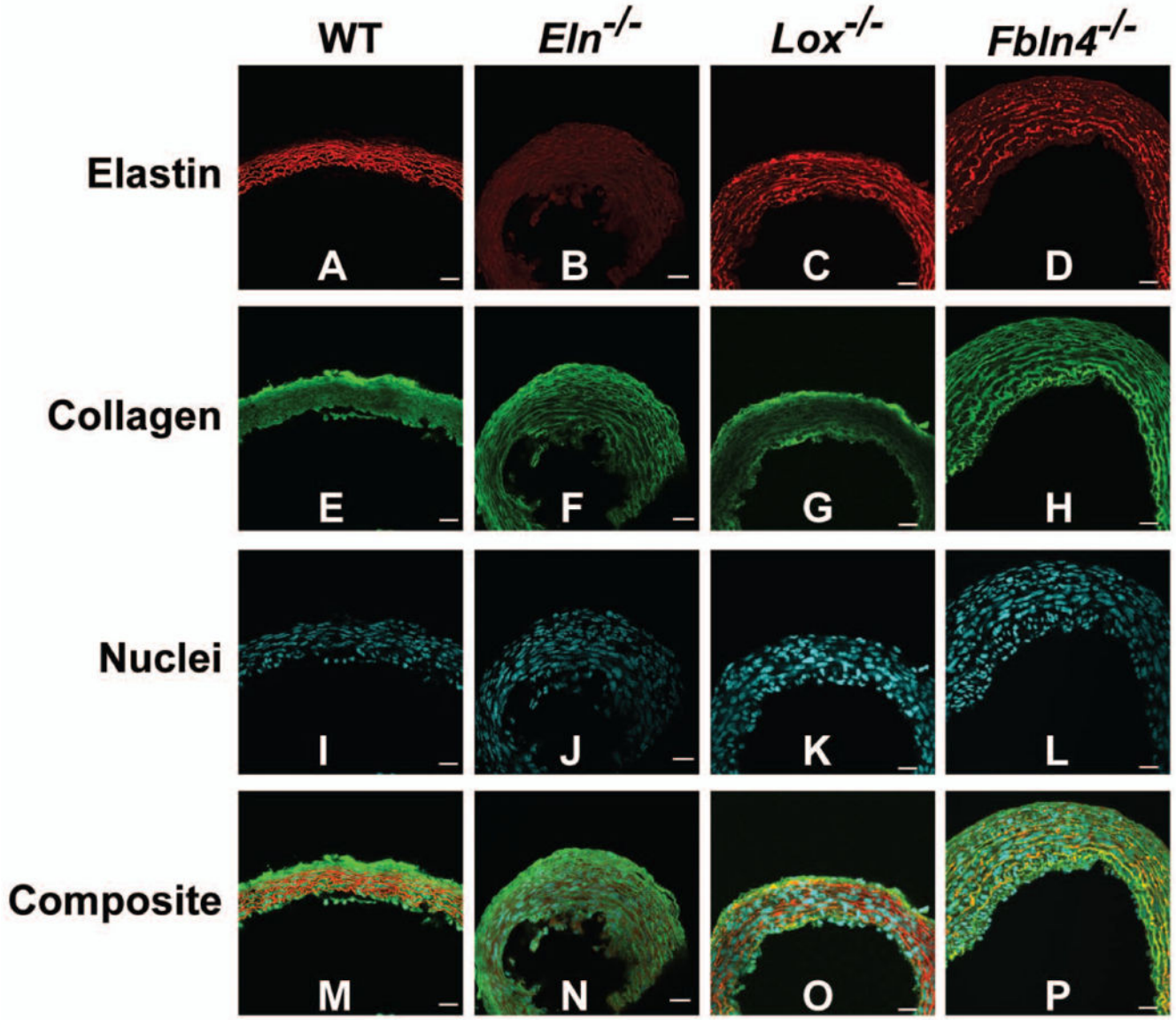

Fig. 4.

Cross-sectional images of newborn AAs. Elastin is red, collagen is green, and cell nuclei are cyan. Elastic lamellae are uninterrupted in WT AA, absent in *Eln*$^{-/-}$ AA, and fragmented in *Lox*$^{-/-}$ and *Fbln4*$^{-/-}$ AA (A – D). Collagen appears normal in KO AAs (E – H). The cell density is similar across groups, but the nuclei appear disorganized near the lumen of KO AAs (I – L). Composite images are shown in panels M – P. The lumen is at the bottom of the images. Scale bar = 20 μm. 3 – 5 aortic sections were examined for each group.

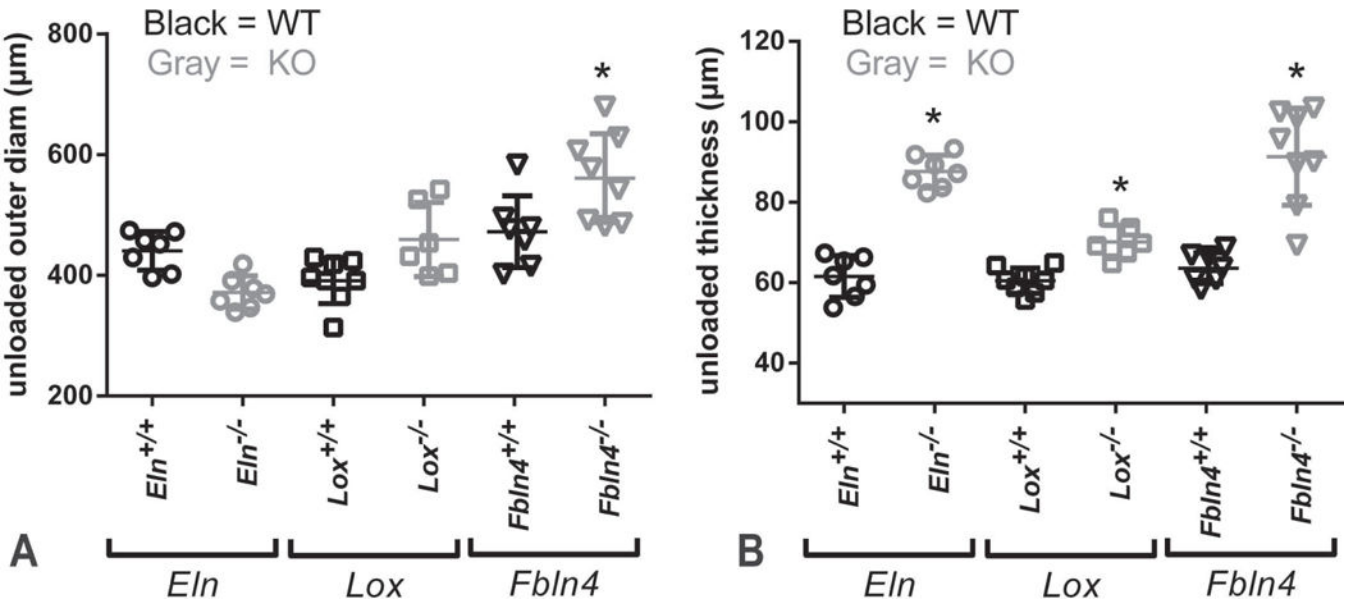

Fig. 5.

Unloaded dimensions for newborn mouse AAs. The outer diameter at a pressure of 0 mmHg is larger in *Fbln4*$^{-/-}$ AA than *Fbln4*$^{+/+}$ (A). The unloaded wall thickness measured from cut rings is larger for all KO AAs than WT (B). * = P < .05. Mean ± SD are shown on the scatter plots. N = 6 – 8/group.

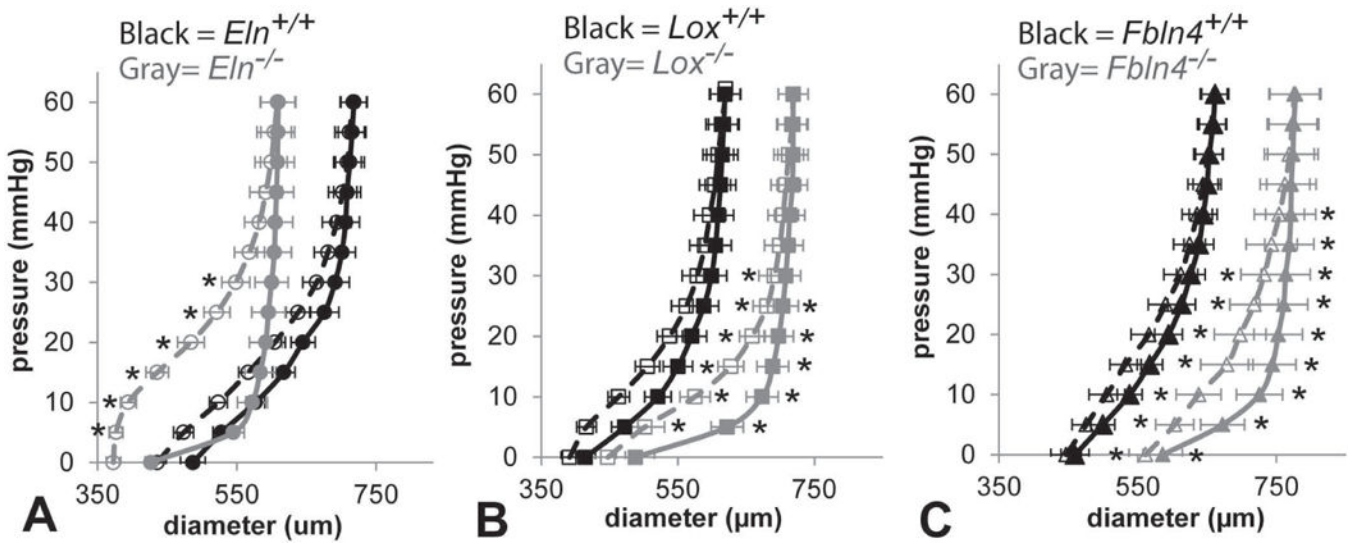

Fig. 6.

Average outer diameter vs. pressure curves for newborn *Eln* (A), *Lox* (B), and *Fbln4* (C) AAs held at 1.05 axial stretch. The average outer diameter was calculated for every 5 mmHg pressure increment. All KO diameters are significantly different from WT at 5 – 30 mmHg for the loading data. $Lox^{-/-}$ and $Fbln4^{-/-}$ AAs show diameter differences from their respective WT controls for the unloading data as well. All KO AAs show larger differences between the loading and unloading behavior than WT. Open symbols, dotted lines = loading. Filled symbols, solid lines = unloading. * = $P < .05$. Mean ± SEM. N = 6 – 8/group.

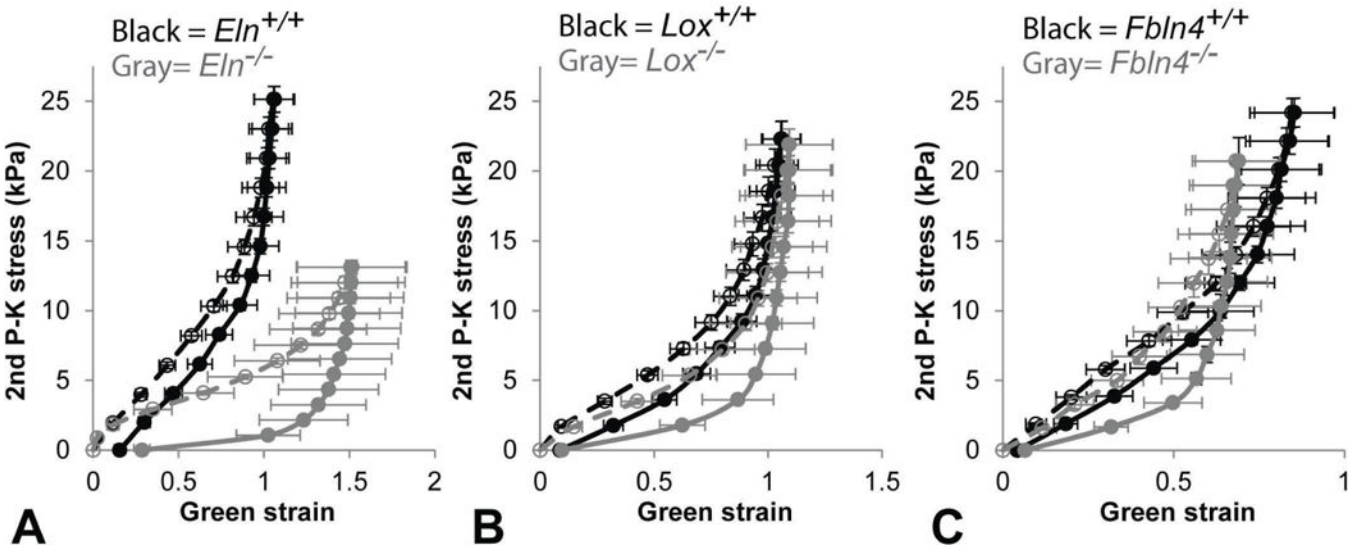

Fig. 7.

Average Green strain vs. second Piola-Kirchoff (2nd P–K) stress curves for newborn *Eln* (A), *Lox* (B), and *Fbln4* (C) AAs pressurized cyclically from 0 – 60 mmHg at 1.05 axial stretch. The average strain and stress were calculated from the outer diameter at every 5 mmHg pressure increment. $Eln^{-/-}$ curve is shifted to the right, $Lox^{-/-}$ curve is similar to, and $Fbln4^{-/-}$ curve is shifted to the left of their respective WT controls. All KO AAs show larger differences between the loading and unloading behavior than WT. Filled symbols, solid lines = unloading. Mean ± SEM. N = 6 – 8/group.

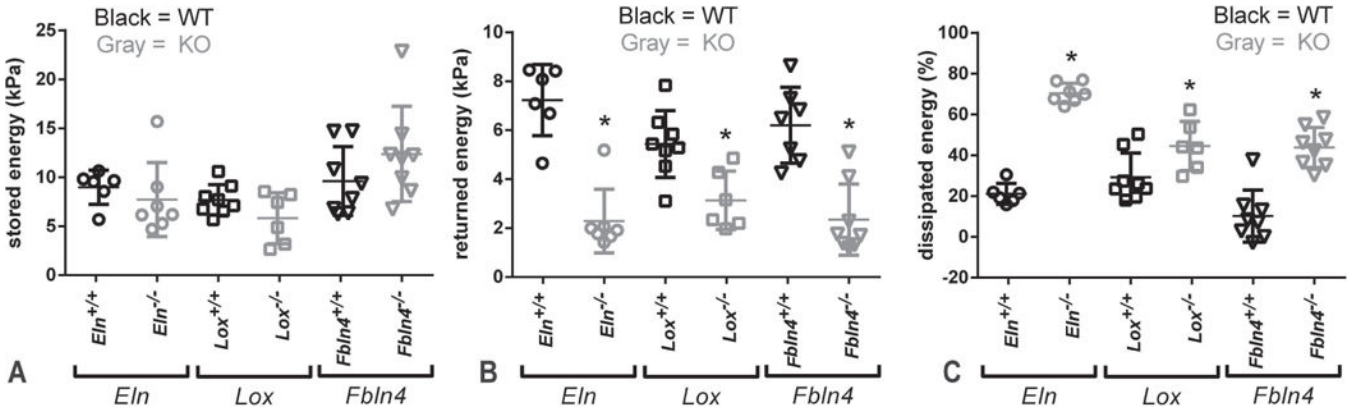

Fig. 8.

Quantification of energy stored, returned, and dissipated for newborn mouse AAs pressurized from 0 – 60 mmHg at 1.05 axial stretch. Stored energy (A) and returned energy (B) are the areas under the loading and unloading Green strain vs. second Piola-Kirchoff stress curves, respectively. Dissipated energy (C) is the percent energy lost during one complete loading and unloading cycle. All KO AAs have significantly reduced returned energy and increased dissipated energy. * = P < .05. Mean and SD are marked in the scatter plots. N = 6 – 8/group.

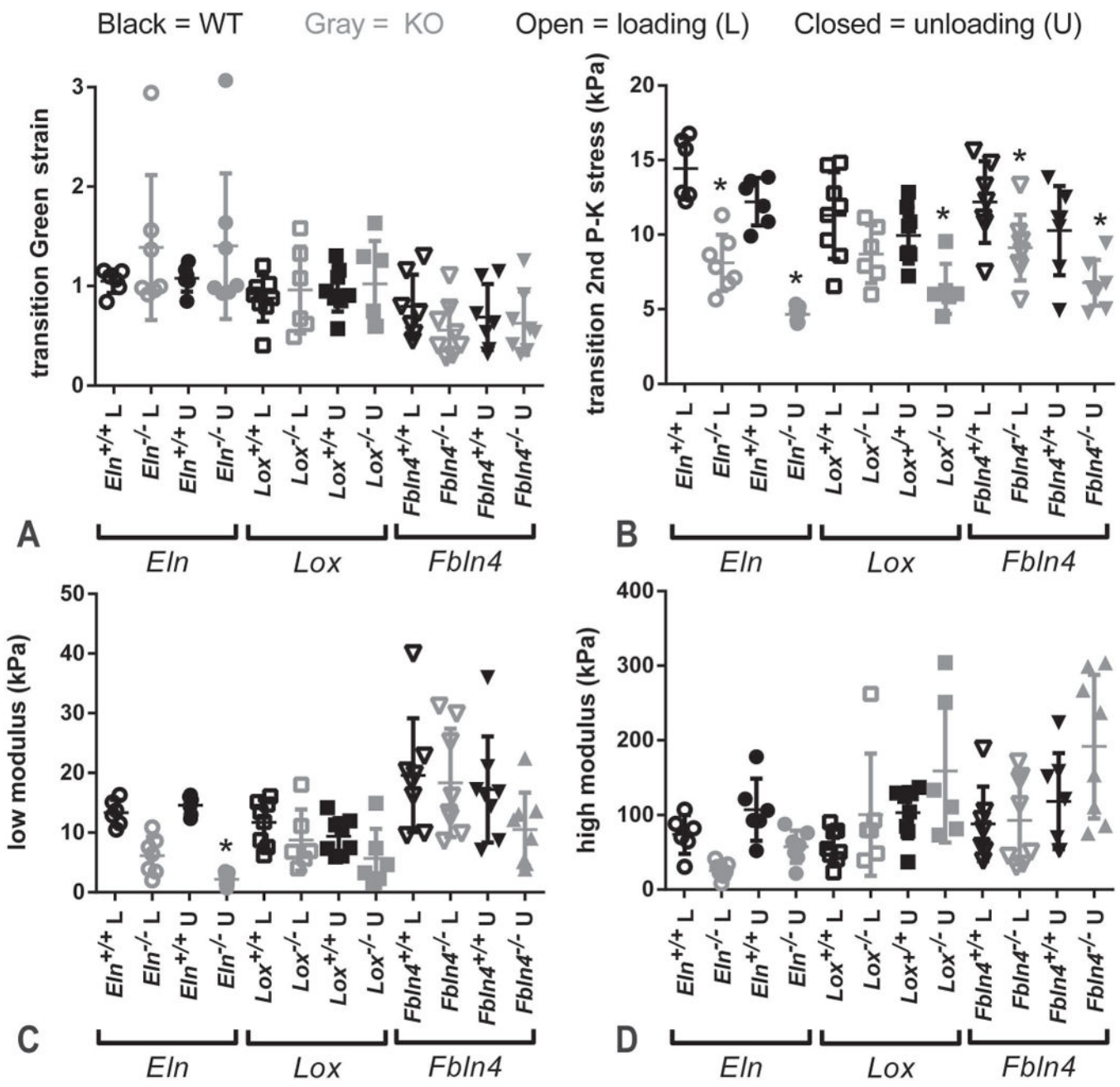

Fig. 9.

Quantification of Green strain vs. second Piola-Kirchoff (2nd P–K) stress curves for newborn mouse AAs. The transition between the low and high modulus values is thought to represent the point at which the AA mechanical behavior shifts from elastin-dominated at low pressure to collagen-dominated at high pressure. The transition Green strain is similar across groups (A). The transition 2nd P–K stress is reduced in most KO groups for loading and unloading (B). The low modulus is decreased only in $Eln^{-/-}$ AA for unloading (C). The high modulus is similar across groups (D). * = P < .05. Mean and SD are marked in the scatter plots. N = 6 – 8/group.

Table 1

Summary of the genetic KO mouse models used in this study. Values for crosslinked elastin and collagen amounts in the AA are listed as a percent change from WT values with arrows indicating the direction of change. Mechanical properties for the loading (L) and unloading (U) data are also listed as a percent change from WT values. A flat line (–) indicates no significant change from WT.

Mouse model	Protein affected	Protein function	Crosslinked Elastin	Collagen	L/U	Trans. strain	Trans. stress	Low modulus	High modulus	Diss. energy
Eln$^{-/-}$	elastin	Major component of elastic fibers in arterial wall	↓ 98%	–	L	–	↓44%	–	–	↑198%
					U	–	↓72%	↓82%	–	
Lox$^{-/-}$	lysyl oxidase	crosslinks elastin and collagen	↓ 56%	–	L	–	–	–	–	↑53%
					U	–	↓36%	–	–	
Fbln 4$^{-/-}$	fibulin-4	involved in elastic fiber assembly and collagen maturation	↓ 84%	–	L	–	↓27%	–	–	↑387%
					U	–	↓41%	–	–	